Oxidative Stress-Induced Dysfunction of Muller Cells During Starvation

Toft-Kehler, Anne Katrine; Gurubaran, Iswariyaraja Sridevi; Madsen, Claus Desler; Rasmussen, Lene Juel; Jensen, Dorte Skytt; Kolko, Miriam

Published in:
Investigative Ophthalmology & Visual Science

DOI:
10.1167/iovs.16-19275

Publication date:
2016

Document Version
Publisher's PDF, also known as Version of record

Oxidative Stress-Induced Dysfunction of Müller Cells During Starvation

Anne Katrine Toft-Kehler,[1] Iswariaraja Scridevi Gurubaran,[1] Claus Desler,[2] Lene J. Rasmussen,[2] Dorte Marie Skytt,[1] and Miriam Kolko[1–3]

[1]Department of Neuroscience and Pharmacology, University of Copenhagen, Copenhagen, Denmark
[2]Center of Healthy Aging, Department of Cellular and Molecular Medicine, University of Copenhagen, Copenhagen, Denmark
[3]Department of Ophthalmology, Zealand University Hospital, Roskilde, Denmark

Correspondence: Miriam Kolko, Department of Ophthalmology, Zealand University Hospital, Vestermarksvej 23, 4000 Roskilde, Denmark; mkolko@dadlnet.dk.

Submitted: February 2, 2016
Accepted: April 1, 2016

Citation: Toft-Kehler AK, Gurubaran IS, Desler C, Rasmussen LJ, Skytt DM, Kolko M. Oxidative stress-induced dysfunction of Müller cells during starvation. *Invest Ophthalmol Vis Sci*. 2016;57:2721–2728. DOI:10.1167/iovs.16-19275

Purpose. Müller cells support retinal neurons with essential functions. Here, we aim to examine the impact of starvation and oxidative stress on glutamate uptake and mitochondrial function in Müller cells.

Methods. Cultured human retinal Müller cells (MIO-M1) were exposed to H_2O_2 and additional starvation for 24 hours. Effects of starvation and H_2O_2 on glutamate uptake and mitochondrial function were assessed by kinetic glutamate uptake assays and Seahorse assays, respectively. Cell survival was evaluated by cell viability assays. mRNA and protein expressions were assessed by quantitative PCR and Western blot.

Results. Starvation of Müller cells increased the glutamate uptake capacity as well as the expression of the most abundant glutamate transporter, *EAAT1*. Mitochondrial and glycolytic activity were diminished in starved Müller cells despite unaffected cell viability. Simultaneous starvation and exposure to oxidative stress resulted in a reduced glutamate uptake and a collapsed mitochondrial function. In Müller cells with intact energy supply, the glutamate uptake and mitochondrial function were unaffected after exposure to oxidative stress.

Conclusions. Here, we identify an increased susceptibility toward oxidative stress in starved Müller cells in spite of unaffected viability and an apparent decreased ability to transport glutamate. Solely exposure to oxidative stress did not affect Müller cell functions. Thus, our study suggests an increased susceptibility of Müller cells in case of more than one cellular stressor. Extrapolating these findings, age-related neurodegenerative retinal diseases may be the result of impaired Müller cell function.

Keywords: Müller cells, starvation, oxidative stress, glutamate uptake, mitochondrial function

Increasing evidence has highlighted the involvement of oxidative stress in the progressive retinal ganglion cell (RGC) death characterizing neurodegeneration in the retina.[1,2] Since oxidative stress involves dysfunctional mitochondrial activity,[3–6] the interplay between energy metabolism and oxidative stress becomes an important matter to explore. In the inner retina, exchange of energy sources occurs through a close interaction between the vasculature, the Müller cells, and the inner retinal neurons.

Müller cells are the predominant glial cell type in the retina. They span the entire thickness of the neuroretina and surround all retinal neurons.[7] The anatomical position is reflected by a multitude of functional interactions between Müller cells and RGCs.[8,9] In addition to the close proximity between Müller cells and RGCs, Müller cells are interposed between the vasculature and the neurons. This morphological relationship leads to important roles of Müller cells in the metabolic symbiosis between the Müller cells and RGCs.

In recent years, the implications of the neuro-glia interaction in the retina has been established, and growing literature suggests important roles of Müller cells in the maintenance of RGCs.[9,10] One of the key roles of Müller cells is to protect RGCs by the uptake and degradation of the neurotransmitter and excitotoxin glutamate.[11] More studies have implicated excessive glutamate levels in the pathogenesis of the most common neurodegenerative retinal disease, glaucoma.[12–14] Furthermore, a study has reported diminished neurotoxic effects of glutamate on RGCs in the presence Müller cells.[15] Thus, increasing literature has shown important roles of Müller cells in RGC survival, and evidence has further indicated that metabolic stressed Müller cells display a disturbance of retinal glutamate metabolism followed by neuronal cell death.[13,15,16]

The present study aims to provide a more profound understanding of the complex and causal interplay between oxidative stress and altered energy supply related to Müller cell function. We hypothesize that Müller cells exposed to oxidative stress and starvation become dysfunctional followed by altered metabolic and neuroprotective properties. Our novel findings illustrate that oxidative stress contributes to disturbed glutamate uptake and energy metabolism in Müller cells. These findings confirm the hypothesis of neuro-glia interactions being a crucial pathogenic element in neurodegenerative retinal diseases.[17,18]

Methods

Cell Culture

Experiments were performed using the human Müller glial cell line MIO-M1,[19] kindly provided by Astrid Limb, University College London, United Kingdom. Müller cells were maintained at 37°C in a humidified chamber of 5% CO_2 in Dulbecco's

Table. Primer Sequences for Quantitative Real-Time PCR for Constitutive Genes

	Primers for Quantitative Real-Time PCR		
Gene	Forward Primer	Reverse Primer	Reference Sequence
EAAT1	5′-CTCACAGTCACCGCTGTCAT-3′	5′-TGTTTTCCTTTGTGCCCTTC-3′	NM 001166696.2
SOD1	5′-TGGCTTGTGGTGTAATTG-3′	5′-TAGCAGGATAACAGATGAGT-3′	NM 000454.4
GAPDH	5′-AGCCTCAAGATCATCAGCAATGCC-3′	5′-TGTGGTCATGAGTCCTCCCACGAT-3′	NM 001289746.1

modified Eagle's medium (DMEM) containing 4.5 g/L glucose, 1 mM pyruvate, 3.97 mM L-glutamine (Gibco by Life Technologies, Carlsbad, CA, USA) supplemented with 10% fetal calf serum (Biological Industries, Beit-Haemek, Israel), 90 Units/mL penicillin and 90 μg/mL streptomycin (Gibco by Life Technologies). The Müller cells were grown in tissue culture flasks or plates (TPP, Trasadingen, Switzerland) to confluency of 80% to 90%, and the culture medium was replaced with fresh medium twice a week. Passages used were 24 to 29. During experiments, Müller cells were maintained in DMEM as described above with glucose, pyruvate, or L-glutamine. This condition is referred to as control (ctrl) in the figures. The condition without glucose, pyruvate, or L-glutamine is referred to as starvation. Induction of oxidative stress was performed with hydrogen peroxide (H_2O_2; Sigma-Aldrich Corp., St. Louis, MO, USA) in concentration of 100 μM. Cells were treated with the described conditions for either 1 hour or 24 hours.

MTT

Cell viability was determined by the colorimetric method, MTT (3-(4,5-dimethyl-2-thiazolyl)-2,5-diphenyl-2H-tetrazolium bromide) measuring the ability of viable cells to reduce MTT to a purple formazan salt. MTT was measured as absorbance at 560 nm. The background readings (blank wells with medium, MTT, and solubilization buffer) were subtracted from the average absorbance readings of the treated wells to obtain an adjusted absorbance reading that represented the cell viability. Subsequently, the readings were divided by the adjusted absorbance readings of untreated cells to obtain the percentage of cell survival.

Lactate Dehydrogenase

Lactate dehydrogenase (LDH) cell cytotoxicity kit (Takara Bio, Inc., Shiga, Japan) was used to quantitatively assess cell survival. Lactate dehydrogenase-release was assayed by measuring absorbance at 490 nm. Cell survival was calculated based on the supernatants, before and after treating the cells with Triton-X 1%. The calculations followed the same method as in the MTT assay.

Quantitative Real-Time PCR

The 80% to 90% confluent MIO-M1 cultures were treated with different conditions as mentioned in the previous section. According to the manufacturer's protocol, total RNA was isolated using the Nucleospin RNA II kit (Macherey Nagel, Düren, Germany). The integrity of total RNA was checked by running the samples in a 1% agarose gel, and intact 18S and 28S ribosomal RNA were observed. The purity of RNA was measured using NanoDrop1000 Spectrophotometer (Thermo Scientific, Waltham, MA, USA). To synthesize cDNA from total RNA, equal amounts of RNA were reverse-transcribed using High Capacity RNA to cDNA kit (Applied Biosystems, Foster City, CA, USA) under the following conditions: incubation at 37°C for 60 minutes and inactivation at 95°C for 5 minutes. Quantitative PCR was performed using the SYBR Select Master Mix (Applied Biosystems), and thermal cycling conditions comprised 40 cycles of denaturation at 95°C for 15 seconds and annealing/extension at 60°C for 1 minute. Quantitative PCR was carried out on a StepOnePlus real-time PCR System (Applied Biosystems). All primers were selected from previously published peer-reviewed papers, and their specificity was analyzed using BLAST. The primer sequences are listed in the Table. The melt curve analysis was performed using StepOne Software version 2.3. The relative expression of each gene was normalized with *GAPDH* reference gene. Statistical analysis of relative gene expressions was evaluated by the comparative ΔΔCt method.[20] Minimum information for publication of quantitative Real-Time PCR experiments (MIQE) guidelines were adopted during the entire experiment.[21]

Western Blot Analysis

The 80% to 90% confluent MIO-M1 cultures were collected and centrifuged at 550*g* for 5 minutes at 4°C and lysed in 100 μL radioimmune precepitation assay buffer (RIPA) buffer (Sigma-Aldrich Corp.) including protease inhibitor cocktail 1 (Sigma-Aldrich Corp.) and protease inhibitor cocktail 2 (Sigma-Aldrich Corp.). Samples were centrifuged at 8000*g* for 10 minutes at 4°C, and samples containing 25 μg proteins were loaded onto gels for investigating the expression of the excitatory amino acid transporter (EAAT1; Abcam, Cambridge, UK) and superoxide dismutase 1 (SOD1; Sigma-Aldrich Corp.). Blots were preincubated for 1 hour with Tris-buffered saline (TBS) (20 mM Tris-HCl, 150 mM NaCl) containing 5% nonfat dry milk and incubated with primary antibodies against EAAT1 (dilution 1:200) and SOD1 (1:500) in TBS 1% nonfat dry milk over night at 4°C. Blots were washed in TBS and incubated with goat anti-rabbit IgG alkaline phosphatase conjugated secondary antibody (Jackson ImmunoResearch, West Grove, PA, USA) followed by visualization using BCIP/NBT (5-bromo-4-chloro-3-indoyl phosphate-nitroblue tetrazolium) substrate (Kirkegaard & Perry Laboratories, Gaithersburg, MD, USA). To ensure that equal quantities were loaded in each lane, the membranes were incubated with GAPDH antibody at dilution 1:1000 (Cell Signaling Technologies, Danvers, MA, USA). Immunoreactive bands were quantified by densitometry (Fiji; ImageJ software, National Institutes of Health, Bethesda, MD, USA), and the density of each band was normalized to its own GAPDH.

Glutamate Uptake Assay

The kinetic characterization of glutamate transport into the Müller cells was performed as described in our previous study.[16] Briefly, MIO-M1 cells were cultured in 24-well plates, and the cells were treated with the relevant condition for 1 or 24 hours. The cells incubated for 3 minutes at 37°C in HEPES buffered saline solution (HBSS; 142 mM NaCl, 5.0 mM KCl, 1.0 mM $CaCl_2$, 1.0 mM $MgCl_2$, 1.0 mM Na_2HPO_4, and 10 mM HEPES) containing different concentration of L-glutamate (range 1–50 μM). Subsequently, the MIO-M1 cells incubated for a further 3 minutes in HBSS including trace amounts of L-

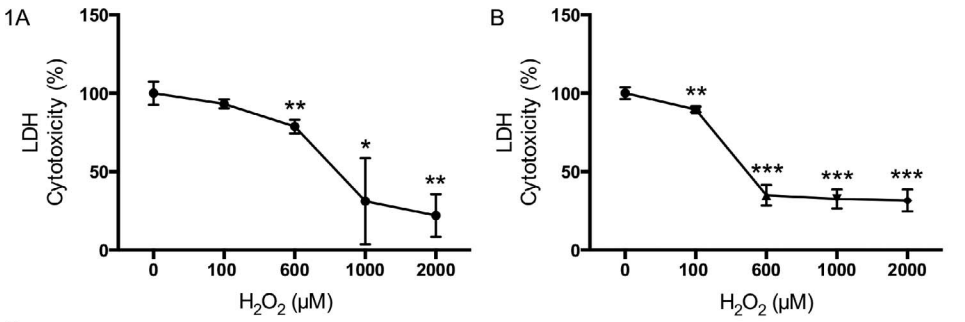

C

Cell Survival	Ctrl	Starvation	Ctrl	H_2O_2	Ctrl (Starvation)	H_2O_2
LDH						
1 H	100 ±15.5	101 ±14.0	100 ±15.5	106 ±12.1	100 ±14.2	109 ±12.2
24 H	100 ±10.4	71 ±21.4	100 ±7.4	93 ±2.9	100 ±3.7	90 ±1.8
MTT						
1 H	100 ±9.0	98 ±13.1	100 ±9.0	102 ±17.1	100 ±2.9	85 ±5.7
24 H	100 ±2.3	75 ±14.4	100 ±2.3	112.8 ±3.5 *	100 ±1.2	59 ±17.3

Figure 1. The cytotoxic effect of H_2O_2 on Müller cells. Müller cells were cultured in presence or absence of energy for 24 hours (**A** and **B**, respectively) and the cytotoxic effect of H_2O_2 at different micromolar concentrations was measured. Values are presented as mean percentage ± SEM of three to four experiments. $^*P < 0.05$, $^{**}P < 0.01$, and $^{***}P < 0.001$. The subtoxic concentration of H_2O_2 (100 μM) used in the present study was further evaluated by LDH and MTT assays (**C**). Values are presented as mean percentage ± SEM of three to four experiments. $^*P < 0.05$.

[3,4-^{3}H]-glutamate (4 μCi/mL, Perkin-Elmer, Waltham, MA, USA). The cellular content of radioactivity was determined in the potassium hydroxide (KOH) extracts and analyzed by liquid scintillation counting in a Beckman LS6500 Liquid Scintillation Counter (Beckman Coulter, Brea, CA, USA). Uptake rates were corrected for protein concentrations, which were measured in the cell extracts using BCA protein assay kit (Sigma-Aldrich Corp.). Unspecific uptake was determined by incubation at 0°C. Uptake kinetics was assumed to follow normal Michaelis-Menten kinetics. The Michaelis-Menten constant, K_m, and the maximal uptake rate, V_{max}, were determined using nonlinear regression in GraphPad Prism 6 (GraphPad Software, La Jolla, CA, USA; $y = V_{max} \cdot x / (K_m + x)$).

Determination of Mitochondrial Bioenergetics

Mitochondrial bioenergetics of MIO-M1 cells was measured using an XF24 Extracellular Flux Analyzer (Seahorse Bioscience, North Billerica, MA, USA). Cells were plated with a density of 250.000 cells per well in a XF24 cell culture microplate (Seahorse Bioscience) and grown over night to ensure plating. Cells were treated as previously described. Subsequently, all wells were thoroughly washed with Seahorse assay media (Seahorse Bioscience) to ensure complete removal of H_2O_2. Cells were incubated in a CO_2 free incubator at 37°C for 1 hour to allow temperature and pH equilibration, after which the microplate including the cells was loaded into the XF24. Measurements of oxygen consumption rate (OCR), as well as extracellular acidification rate (ECAR) of each well was done over a period of 80 minutes. As H_2O_2 degrades to H_2O and O_2, great caution was taken to wash cells and thereby to minimize the impact on OCR measurements. The adenosine 5′-triphosphate (ATP) synthase inhibitor oligomycin (1 μM), the uncoupler carbonyl cyanide-4-(trifluromethoxy)phenylhydrazone (FCCP; 4 μM) and the complex III inhibitor antimycin A (2 μM) was added to each well after 20, 40, and 60 minutes, respectively. This allowed the determination of basal ATP turnover (difference in OCR before and after addition of oligomycin, as per Supplementary Fig.), maximal respiration (difference in OCR before and after addition of FCCP), and basal glycolysis.

ATP Assay

Intracellular ATP concentrations were measured using the Bioluminescent Somatic Cell Assay Kit (Sigma-Aldrich Corp.) per manufacturer's protocol. A TopCount NXT microplate scintillation and luminescence counter (Perkin-Elmer) was used to measure the luminescence signal from samples in opaque white 96-well plates (TPP). Adenosine 5′-triphosphate standards (Sigma-Aldrich Corp.) were used to create an ATP calibration curve for the assay.

Statistics

Statistical analysis was performed using graphing and statistical software (GraphPad Prism; GraphPad Software) and P values less than 0.05 were considered significant. The sample size of each experiment (n) was determined from either a triplicate or more. All data are expressed as means ± SEM and differences between conditions were analyzed using paired and unpaired 2-tailed t-tests and multiple t-tests.

Results

Cell Viability Experiments Confirmed the Subtoxic Level of H_2O_2

With the aim to determine the subtoxic concentration of H_2O_2 on Müller cell function, we measured the cytotoxic effect of H_2O_2 at different concentrations ranging from 0 to 2000 μM in cultures with sufficient energy availability, as well as in cultures starved from energy sources (Figs. 1A, 1B, respectively). Our study revealed an increased sensitivity to H_2O_2 in starved cultures and the median lethal dose (LD50) changed from approximately 1000 μM H_2O_2 in cultures with sustained energy supply (Fig. 1A) to 600 μM H_2O_2 in starved cultures

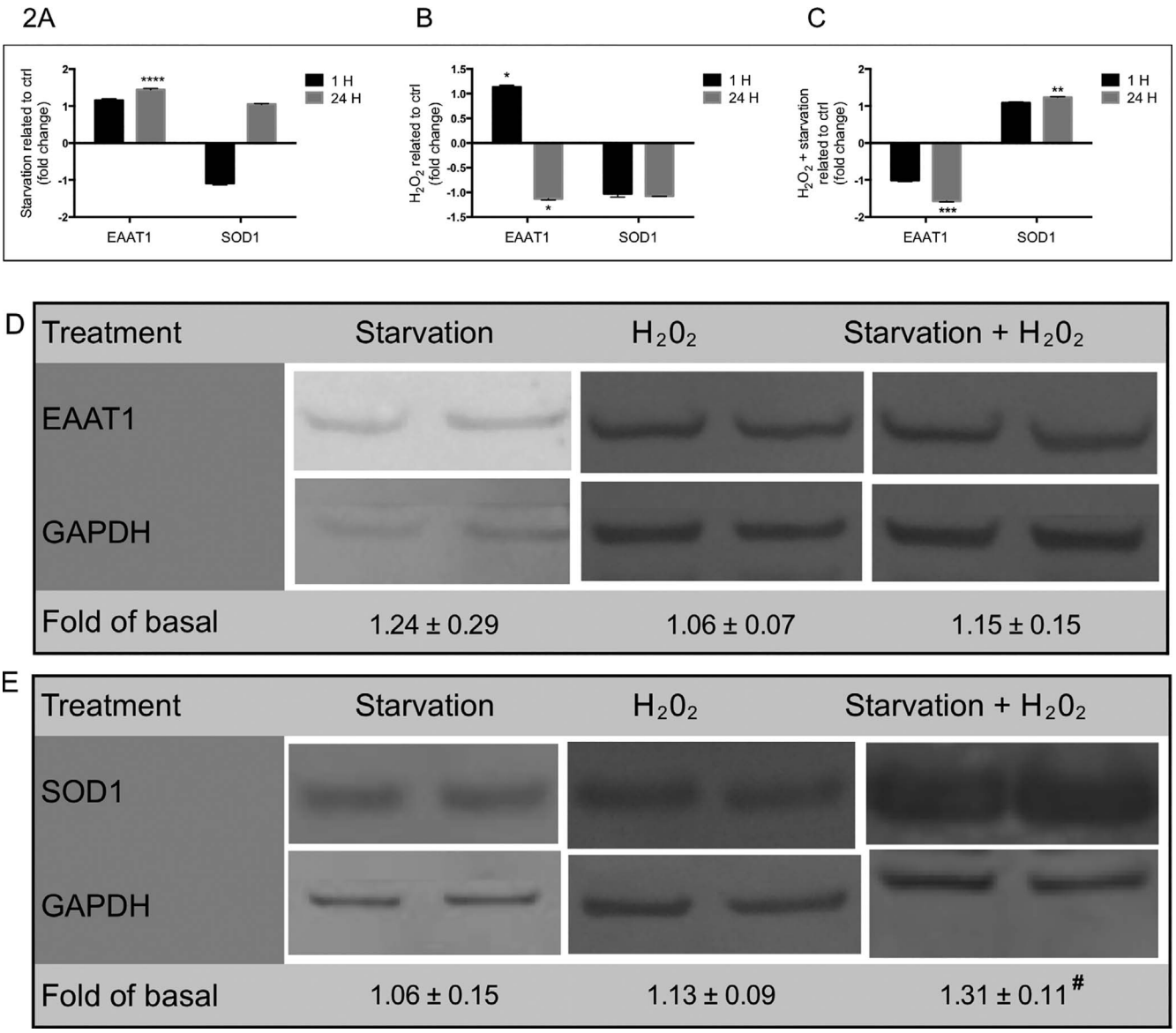

Figure 2. Müller cell mRNA expression of *EAAT1* and *SOD1* in response to starvation, H_2O_2, or combined starvation and H_2O_2 (**A–C**). After 1 hour or 24 hours of treatment (*black and grey bars*, respectively) the RNA was extracted from the cells and analyzed by quantitative real-time PCR. Control (ctrl) indicates normal Müller cells (**A**, **B**) or starved Müller cells (**C**). Values are presented as relative means ± SEM of 3 to 18 experiments. $^{*}P < 0.05$, $^{**}P < 0.01$, $^{***}P < 0.001$, and $^{****}P < 0.0001$. Müller cell protein expression during starvation, during H_2O_2, and combined starvation and H_2O_2 (**D**, **E**). Changes of EAAT1 and SOD1 expression were measured by Western blot analysis in response to 1 hour or 24 hours of treatment. A representative blot of $n = 3$ is shown. Control (ctrl) indicates normal Müller cells (compared with starvation and H_2O_2) or starved Müller cells (compared with simultaneous starvation and treatment with H_2O_2). Values are presented as relative means ± SEM. $^{\#}P = 0.054$.

(Fig. 1B). Based on these experiments, we decided to use a subtoxic concentration of 100 µM H_2O_2 in subsequent experiments. Additionally, we did a comprehensive cell survival experiment by LDH and MTT to confirm that the Müller cells would tolerate the conditions and timeframes used in the study (Fig. 1C).

Differential Regulation of mRNA and Proteins in Müller Cells in Response to Oxidative Stress and Starvation

To evaluate a potential regulation of glutamate transporters and the antioxidant defense system in response to starvation and oxidative stress, we determined the expression of the most abundant EAAT1, and the antioxidant enzyme, SOD1. Gene expression of *EAAT1* was significantly up regulated in response to 24 hours of starvation (Fig. 2A; 1.44-fold, $P < 0.0001$). The Western blot analysis supported a tendency toward an increased expression of EAAT1 (Fig. 2D; 1.24-fold). In contrast, *EAAT1* was significantly down regulated on mRNA level after 24 hours of exposure to H_2O_2 or H_2O_2 and starvation (Fig. 2B; −1.13-fold, $P < 0.05$; Fig. 2C; −1.57-fold, $P < 0.001$).

The antioxidant enzyme *SOD1* was shown to be significantly increased on mRNA level due to 24 hours of simultaneous exposure to H_2O_2 and starvation (Fig. 2C; 1.23-fold, $P < 0.01$). This up regulation was confirmed on protein level, where we found a tendency toward an increased protein expression (Fig. 2E; 1.31-fold, $P = 0.054$).

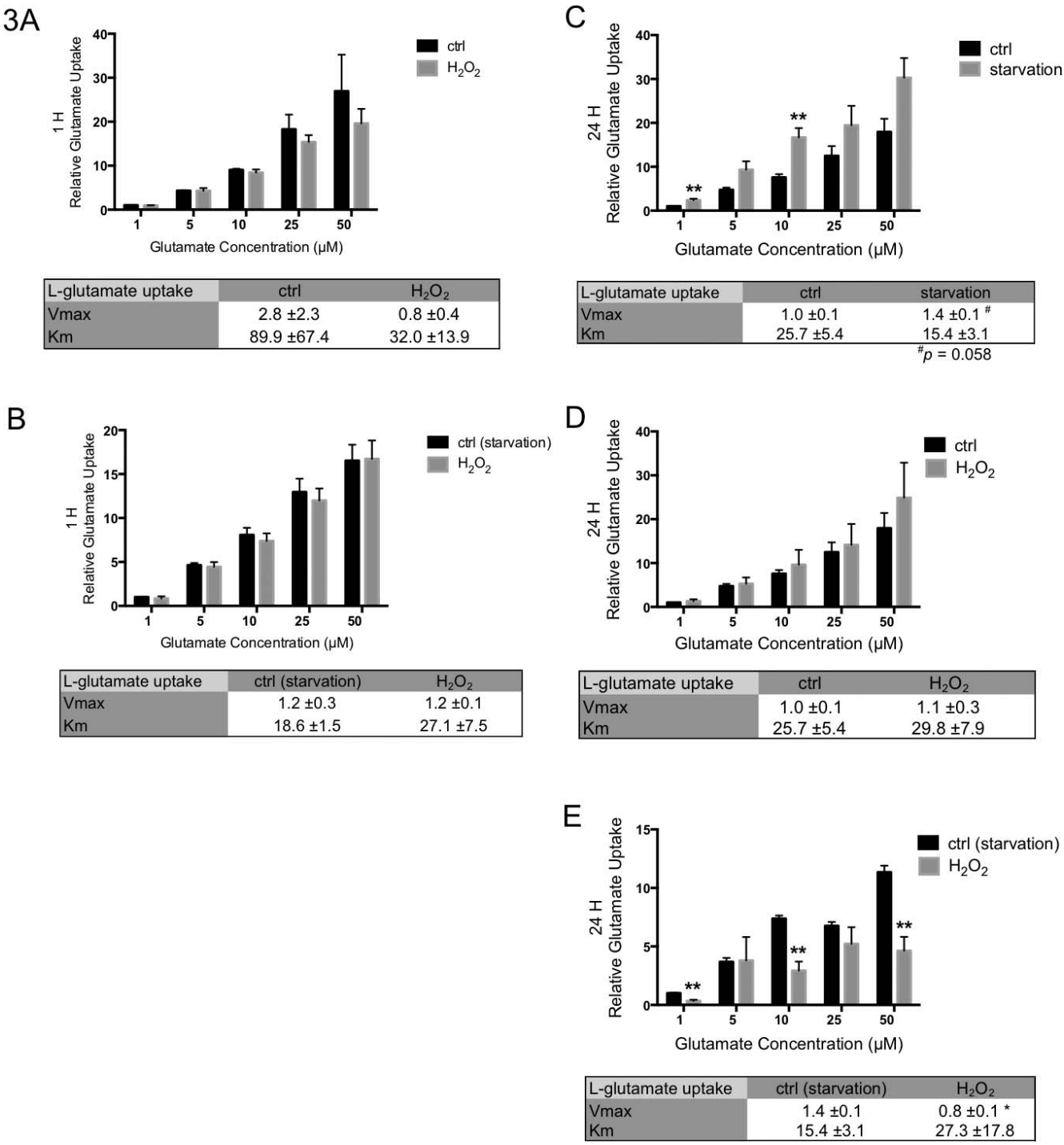

L-glutamate uptake	ctrl	H_2O_2
Vmax	2.8 ±2.3	0.8 ±0.4
Km	89.9 ±67.4	32.0 ±13.9

L-glutamate uptake	ctrl	starvation
Vmax	1.0 ±0.1	1.4 ±0.1 #
Km	25.7 ±5.4	15.4 ±3.1

$^{\#}p = 0.058$

L-glutamate uptake	ctrl (starvation)	H_2O_2
Vmax	1.2 ±0.3	1.2 ±0.1
Km	18.6 ±1.5	27.1 ±7.5

L-glutamate uptake	ctrl	H_2O_2
Vmax	1.0 ±0.1	1.1 ±0.3
Km	25.7 ±5.4	29.8 ±7.9

L-glutamate uptake	ctrl (starvation)	H_2O_2
Vmax	1.4 ±0.1	0.8 ±0.1 *
Km	15.4 ±3.1	27.3 ±17.8

Figure 3. Müller cell glutamate uptake in response to starvation, H_2O_2, and simultaneous starvation and H_2O_2. The Müller cells were cultured 1 hour (**A**, **B**) or 24 hours (**C**–**E**) in condition with sufficient energy availability or with decreased energy sources (starvation). In addition, Müller cells were exposed to H_2O_2. Kinetic L-glutamate uptake at extracellular glutamate concentrations from 1 to 50 μM was measured during the described conditions. Control (ctrl) indicates normal Müller cells (**A**, **C**, **D**) or starved Müller cells (**B**, **E**). Values are presented as relative means ± SEM of three experiments. $^{**}P < 0.01$. The V_{max} and the Michaelis constant, K_m, are shown below each graph, and apparent values calculated in Prism from Eadie-Hofstee plots are expressed as nmol × min^{-1} × mg $protein^{-1}$ and μM, respectively. Values are presented as mean ± SEM. $^{*}P < 0.05$.

Starvation-Induced Increase in Glutamate Uptake and Oxidative Stress-Induced Decrease in Glutamate Uptake During Starvation

Our previous study revealed a 1-hour starvation-induced increase in glutamate uptake.[16] In the present study, we aimed to determine the glutamate uptake after 24 hours of sustained starvation. Similar to cells starved for 1 hour, we showed an increased uptake of glutamate, which was significant at concentrations 1 and 10 μM glutamate (Fig. 3C; $P < 0.01$). Moreover, we found a tendency toward an increased V_{max},

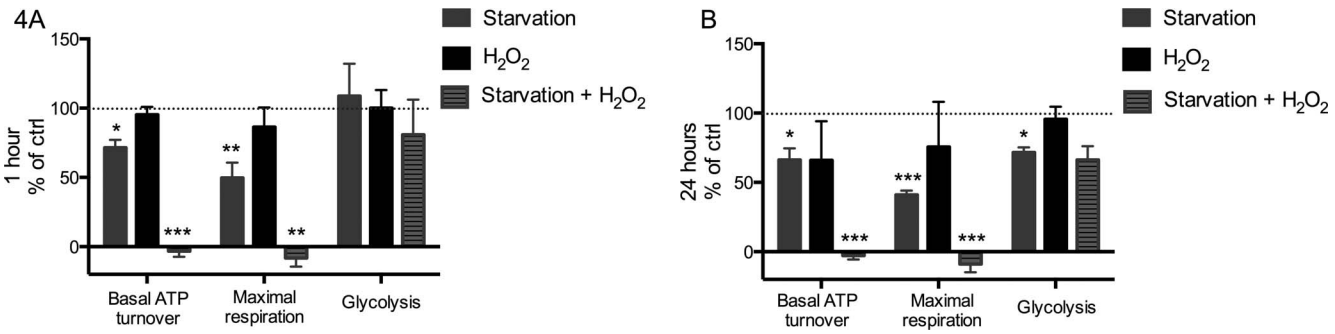

Figure 4. The mitochondrial ATP turnover, the mitochondrial maximal respiration, and the cytosolic glycolysis in Müller cells during starvation and treatment with H_2O_2. The Müller cells were starved for 1 and 24 hours and treated with or without H_2O_2. The intracellular metabolic parameters were quantified as mean percentage ± SEM of three experiments. (**A**, **B**) The intracellular metabolic parameters after 1 and 24 hours of treatment, respectively. Starved cells and cells treated with H_2O_2 were related to a control of normal Müller cells, whereas simultaneous starvation and H_2O_2 was related to a control of starved cells. $^*P < 0.05$, $^{**}P < 0.01$, and $^{***}P < 0.001$.

although not significant (Fig. 3C; $P = 0.058$), whereas K_m remained unchanged.

Simultaneous starvation and treatment of Müller cells with oxidative stress for 24 hours resulted in a significant decrease in the glutamate uptake (Fig. 3E; $P < 0.01$), as well as a significantly decreased V_{max} (Fig. 3E; $P < 0.05$). As shown in Figure 3D, treatment of Müller cells with H_2O_2 alone did not affect the glutamate uptake. The K_m values remained unchanged throughout the experiment.

Oxidative Stress-Induced Alterations of the Mitochondrial Function During Starvation and Oxidative Stress

To determine the effect of starvation and H_2O_2 treatment on mitochondrial bioenergetics, Müller cells were treated with H_2O_2 for 1 and 24 hours during either intact energy supply or during starvation. Starvation reduced basal ATP turnover to 71% and 66% compared to control (Figs. 4A, 4B; $P < 0.05$) after 1 and 24 hours, respectively. Concomitantly, maximal respiration was reduced to 50% and 41% compared to control (Figs. 4A, 4B; $P < 0.01$ and $P < 0.001$, respectively). Simultaneous treatment with starvation and oxidative stress resulted in a complete collapse of the oxidative phosphorylation, where neither ATP turnover nor maximal respiration was measurable (Figs. 4A, 4B; $P < 0.001$ and $P < 0.01$). Müller cells treated with H_2O_2 and grown in cultures with sufficient energy availability did not affect the basal ATP turnover, maximal respiration, or basal glycolysis (Figs. 4A, 4B). In contrast, basal glycolysis was reduced to 72% (Fig. 4B; $P < 0.05$) in response to 24 hours of starvation. A tendency toward a reduction of glycolysis was found due to simultaneous treatment with H_2O_2 and starvation, though not significant (Fig. 4B).

Oxidative Stress-Induced Decrease in ATP Levels During Starvation

The immediate intracellular ATP level was measured after 1 and 24 hours of starvation, exposure to oxidative stress, or both. The latter condition resulted in a significant reduction of the ATP level in Müller cells to 0.60-fold and 0.67-fold in response to both 1 and 24 hours of treatment (Fig. 5B; $P < 0.01$ and $P < 0.001$). Starvation and oxidative stress alone did not affect the intracellular ATP level (Fig. 5A).

Discussion

The present study demonstrates that simultaneous starvation and exposure to oxidative stress diminish the transport of glutamate into Müller cells and reduce the mitochondrial respiration. Moreover, starvation increases the uptake of glutamate and induces increased expression of the most abundant glutamate transporter EAAT1.

The present experiments extend the previous findings concerning Müller cells' impact on inner retinal homeostasis during altered energy supply and oxidative stress. Xie et al.[22] have demonstrated a decreased glutamate uptake and impaired EAAT1 expression in response to high-glucose conditions. Moreover, a study by Dai et al.[23] reported an increased EAAT1

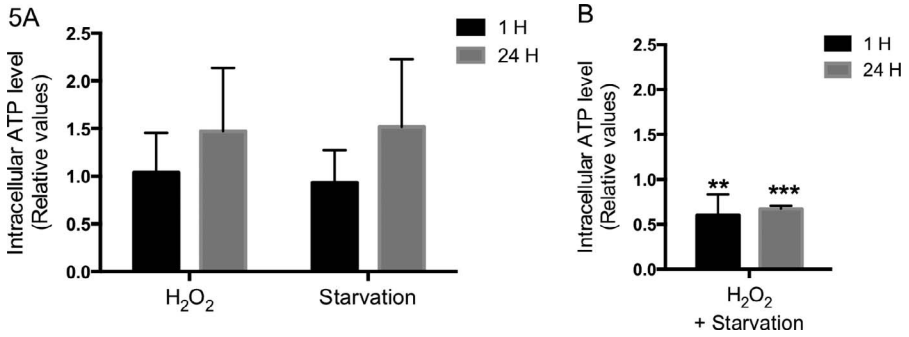

Figure 5. The intracellular levels of ATP in Müller cells in response to starvation, H_2O_2, and combined starvation and H_2O_2. The Müller cells were treated for 1 hour or 24 hours (*black bar and grey bar*, respectively) and intracellular ATP levels were quantified as relative means ± SEM of three experiments. Starved cells and cells treated with H_2O_2 were related to a control of normal Müller cells (**A**), whereas simultaneous starvation and H_2O_2 related to a control of starved cells (**B**). $^{**}P < 0.01$ and $^{***}P < 0.001$.

expression in early-stage hypoxic conditions, though the expression decreased over time. We have previously shown a significantly increased glutamate uptake and significantly increased EAAT1 expression in response to 1-hour starvation.[16] In accordance with our previous study, we now illustrate a sustained increase in glutamate uptake due to starvation for 24 hours and a tendency toward a sustained increase in the expression of EAAT1. Our previous and present results identify an energy-dependent regulation of glutamate uptake. Based on these findings, we suggest that Müller cells have a potential ability to increase glutamate uptake during stressful conditions, which confirm the potential protective role of Müller cells in preventing RGC death. Accordingly, a study by Kawasaki et al.[15] found a protective effect of Müller cells on RGC excitotoxicity.

In addition to energy availability, oxidative stress has been implicated in neurodegenerative retinal conditions.[4,24] In order to exploit oxidative stress-induced dysfunction of Müller cells, our present study demonstrates a synergistic impairment of glutamate uptake, when starved Müller cells are exposed to oxidative stress. Nevertheless, Müller cells with intact energy supply are unaffected by oxidative stress.

When translating our present results into understanding its implications in inner retinal neurodegeneration, comprehensive literature has correlated impaired autoregulation of the retina with increased levels of oxidative stress.[4,25,26] In conditions with limited energy supply, this increased level of oxidative stress should then result in loss of RGCs.[9,27] Müller cells have been shown to rely mainly on glycolysis.[28] Our previous study revealed glycogen levels under detection level after just 1 hour of starvation in MIO-M1 cells.[16] This finding potentially explains the significant impact of starvation on the features of MIO-M1 cells in response to 24 hours of starvation. The depletion of glycogen after 1 hour of starvation does not necessarily occur in primary Müller cells, in which the glycogen reserve could be notably different. Hence, a limitation of the present study is clearly related to the use of the human Müller cell line MIO-M1. More extensive studies on primary Müller cell would be required to further characterize the impact of starvation and oxidative stress on Müller cells.

In the present study, we show that simultaneous starvation and exposure to oxidative stress result in a pronounced impairment of the mitochondrial function. Moreover, this condition results in a tendency toward decreased glycolytic activity. The measured levels of basal glycolysis suggest that the reduced production of ATP by mitochondria is not compensated by glycolysis. Rather, starvation and oxidative stress for 24 hours decrease glycolysis, thereby indicating a shortage of substrates for both respiration and glycolysis. Since the oxidative stress-induced reduction of ATP during starvation is not accompanied by significantly increased cell death, the reduction of ATP during starvation is more likely due to a down regulation of the glutamate uptake, since glutamate potentially function as an energy source.[29] The diminished capacity of glutamate transporters was also reflected in the reduced V_{max} value. As ATP production by oxidative phosphorylation was collapsed, the remaining intracellular ATP levels after simultaneous starvation and treatment with oxidative stress should originate from glycolysis (Fig. 5B). These results suggest that Müller cells exposed to oxidative stress become vulnerable to starvation and that such vulnerability may lead to altered neuroprotective properties.

Mitochondrial dysfunction is being increasingly recognized as a potential cause of a number of neurodegenerative diseases including glaucoma,[4] Alzheimer's, Parkinson's, amyotrophic lateral sclerosis, and optic neuropathies.[24,30] In donor eyes from patients with glaucoma, evidence has shown increased levels of oxidative stress and mitochondrial dysfunction.[31] Murine glaucoma models have shown similar results with increased oxidative stress and mitochondrial dysfunction.[32] A recent study from Lascaratos et al.[3] has indicated an increased efficacy of mitochondria in subjects without glaucoma compared to subjects with glaucoma. Hence, the study reveals enhanced ability to resist optic nerve injury in patients with superior mitochondrial properties. Finally, more studies have now identified a systemic defect of the mitochondrial complex-I in lymphoblasts of primary open angle glaucoma patients.[33,34]

One of the particular findings in our study is the synergistic impairment of glutamate uptake in Müller cells after simultaneous starvation and exposure to oxidative stress. Since substantial evidence have indicated that excessive glutamate levels is a causative factor in neurodegenerative retinal diseases, it is enticing to suggest that healthy Müller cells will prevent such excitotoxicity.[12–14] On the contrary, metabolic stressed Müller cells will lack this supportive function due to decreased ability to remove glutamate from the synapse. We observed a robust tendency toward an upregulation of the most abundant glutamate transporter EAAT1 in response to 24 hours of starvation. In accordance with these findings, we previously showed a significant upregulation of EAAT1 even after 1 hour of starvation.[16] Since our data point to a regulatory mechanism of EAAT1 expression, our results cannot exclude alternative explanations such as increased EAAT1 activity, transposition of EAAT1, and involvement of less abundant EAATs such as EAAT2 or EAAT3. In addition, the increased capacity of glutamate transport into the Müller cells might not only depend on the presence of EAAT1 on the actual cell surface, but also on the de novo synthesis of EAAT1.

Our results demonstrate that Müller cells can endure starvation if oxidative stress is absent. However, during simultaneous starvation and oxidative stress, their homeostasis becomes disturbed and their glutamate uptake diminished. We believe that Müller cells hold compensatory mechanisms against starvation as well as oxidative stress. Thus, increased uptake of glutamate during starvation and increased SOD1 expression after simultaneous treatment with oxidative stress and starvation are offsets of disturbed metabolism resulting in a compensatory response. Overall, we hypothesize that Müller cells exposed to oxidative stress and starvation become dysfunctional followed by altered metabolic and neuroprotective properties. In line with this assumption, previous studies have demonstrated essential roles of the glia-neuron partnership as crucial pathogenic elements in glaucoma.[10] Furuya et al.[35] revealed increased viability in cocultures of primary RGCs and Müller cells. Furthermore, a study by Kawasaki et al.[15] showed protection by primary Müller cells against glutamate excitotoxicity on primary RGCs.

In summary, our study highlights disturbed Müller cell functions in response to simultaneous starvation and exposure to oxidative stress. When drawing analogy to neurodegenerative retinal conditions, we cautiously suggest that impaired Müller cell function during metabolic stress could be essential in RGC survival. Therefore, the homeostasis of Müller cells displays potential as a novel target for neuroprotective treatment strategies.

Acknowledgments

The authors thank laboratory technicians Hanne Panduro Olsen, Charlotte Taul Brændstrup and Kathrin Jensen, Department of Neuroscience and Pharmacology, University of Copenhagen, Denmark, for skilful assistance to the study.

Supported by Faculty of Health and Medical Sciences, University of Copenhagen, Denmark; Nordea-fonden, Denmark; Velux Founda-

tion, Denmark; and Fight for Sight, Denmark. The authors alone are responsible for the content and writing of the paper.

Disclosure: **A.K. Toft-Kehler**, None; **I.S. Gurubaran**, None; **C. Desler**, None; **L.J. Rasmussen**, None; **D.M. Skytt**, None; **M. Kolko**, None

References

1. Tezel G. The immune response in glaucoma: a perspective on the roles of oxidative stress. *Exp Eye Res*. 2011;93:178–186.
2. Tezel G. Oxidative stress in glaucomatous neurodegeneration: mechanisms and consequences. *Prog Retinal Eye Res*. 2006; 25:490–513.
3. Lascaratos G, Chau K-Y, Zhu H, et al. Neurobiology of disease. *Neurobiol Dis*. 2015;82:78–85.
4. Chrysostomou V, Rezania F, Trounce IA, Crowston JG. Oxidative stress and mitochondrial dysfunction in glaucoma. *Curr Opin Pharmacol*. 2013;13:12–15.
5. Osborne NN. Mitochondria: their role in ganglion cell death and survival in primary open angle glaucoma. *Exp Eye Res*. 2010;90:750–757.
6. Lascaratos G, Garway-Heath DF, Willoughby CE, Chau K-Y, Schapira AHV. Mitochondrial dysfunction in glaucoma: understanding genetic influences. *Mitochondrion*. 2012;12:202–212.
7. Bringmann A, Pannicke T, Grosche J, et al. Müller cells in the healthy and diseased retina. *Prog Retinal Eye Res*. 2006;25: 397–424.
8. Newman E, Reichenbach A. The Müller cell: a functional element of the retina. *Trends Neurosci*. 1996;19(8):307–312.
9. Bringmann A, Wiedemann P. Müller glial cells in retinal disease. *Ophthalmologica*. 2012;227:1–19.
10. Vecino E, Rodriguez FD, Ruzafa N, Pereiro X, Sharma SC. Glia-neuron interactions in the mammalian retina. *Prog Retinal Eye Res*. 2016;51:1–40.
11. Bringmann A, Pannicke T, Biedermann B, et al. Role of retinal glial cells in neurotransmitter uptake and metabolism. *Neurochem Internat*. 2009;54:143–160.
12. Harada T, Harada C, Nakamura K, et al. The potential role of glutamate transporters in the pathogenesis of normal tension glaucoma. *J Clin Invest*. 2007;117:1763–1770.
13. Martin KRG, Levkovitch-Verbin H, Valenta D, Baumrind L, Pease ME, Quigley HA. Retinal glutamate transporter changes in experimental glaucoma and after optic nerve transection in the rat. *Invest Ophthalmol Vis Sci*. 2002;43:2236–2243.
14. Naskar R, Vorwerk CK, Dreyer EB. Concurrent downregulation of a glutamate transporter and receptor in glaucoma. *Invest Ophthalmol Vis Sci*. 2000;41:1940–1944.
15. Kawasaki A, Otori Y, Barnstable CJ. Müller cell protection of rat retinal ganglion cells from glutamate and nitric oxide neurotoxicity. *Invest Ophthalmol Vis Sci*. 2000;41:3444–3450.
16. Toft-Kehler AK, Skytt DM, Poulsen KA, et al. Limited energy supply in Müller cells alters glutamate uptake. *Neurochem Res*. 2014;39:941–949.
17. De Keyser J, Mostert JP, Koch MW. Dysfunctional astrocytes as key players in the pathogenesis of central nervous system disorders. *J Neurol Sci*. 2008;267:3–16.
18. Allaman I, Bélanger M, Magistretti PJ. Astrocyte-neuron metabolic relationships: for better and for worse. *Trends Neurosci*. 2011;34:76–87.
19. Limb GA, Salt TE, Munro PMG, Moss SE, Khaw PT. In vitro characterization of a spontaneously immortalized human Müller cell line (MIO-M1). *Invest Ophthalmol Vis Sci*. 2002; 43:864–869.
20. Schmittgen TD, Livak KJ. Analyzing real-time PCR data by the comparative CT method. *Nature Prot*. 2008;3:1101–1108.
21. Bustin SA, Benes V, Garson JA, et al. The MIQE guidelines: minimum information for publication of quantitative real-time PCR experiments. *Clin Chem*. 2009;55:611–622.
22. Xie B, Jiao Q, Cheng Y, Zhong Y, Shen X. Effect of pigment epithelium-derived factor on glutamate uptake in retinal Müller cells under high-glucose conditions. *Invest Ophthalmol Vis Sci*. 2012;53:1023–1032.
23. Dai M, Xia X-B, Xiong S-Q. BDNF regulates GLAST and glutamine synthetase in mouse retinal Müller cells. *J Cell Physiol*. 2012;227:596–603.
24. Lin MT, Beal MF. Mitochondrial dysfunction and oxidative stress in neurodegenerative diseases. *Nature*. 2006;443:787–795.
25. Mozaffarieh M, Grieshaber MC, Flammer J. Oxygen and blood flow: players in the pathogenesis of glaucoma. *Molecular Vis*. 2008;14:224–233.
26. Newman EA. Functional hyperemia and mechanisms of neurovascular coupling in the retinal vasculature. *J Cereb Blood Flow Metab*. 2013;33:1685–1695.
27. Tezel G; Fourth ARVO/Pfizer Ophthalmics Research Institute Conference Working Group. The role of glia, mitochondria, and the immune system in glaucoma. *Invest Ophthalmol Vis Sci*. 2009;50:1001–1012.
28. Winkler BS, Arnold MJ, Brassell MA, Puro DG. Energy metabolism in human retinal Müller cells. *Invest Ophthalmol Vis Sci*. 2000;41:3183–3190.
29. Ola MS, Hosoya K-I, LaNoue KF. Regulation of glutamate metabolism by hydrocortisone and branched chain keto acids in cultured rat retinal Müller cells (TR-MUL). *Neurochem Internat*. 2011;59:656–663.
30. Yu-Wai-Man P, Griffiths PG, Chinnery PF. Mitochondrial optic neuropathies - disease mechanisms and therapeutic strategies. *Prog Retinal Eye Res*. 2011;30:81–114.
31. McElnea EM, Quill B, Docherty NG, et al. Oxidative stress, mitochondrial dysfunction and calcium overload in human lamina cribrosa cells from glaucoma donors. *Molecular Vis*. 2011;17:1182–1191.
32. Ju W-K, Kim K-Y, Lindsey JD, et al. Intraocular pressure elevation induces mitochondrial fission and triggers OPA1 release in glaucomatous optic nerve. *Invest Ophthalmol Vis Sci*. 2008;49:4903–4911.
33. Lee S, Sheck L, Crowston JG, et al. Impaired complex-I-linked respiration and ATP synthesis in primary open-angle glaucoma patient lymphoblasts. *Invest Ophthalmol Vis Sci*. 2012;53: 2431–2437.
34. Van Bergen NJ, Crowston JG, Craig JE, Burdon KP, et al. Measurement of systemic mitochondrial function in advanced primary open-angle glaucoma and leber hereditary optic neuropathy. *PLoS One*. 2015;10:e0140919.
35. Furuya T, Pan Z, Kashiwagi K. Role of retinal glial cell glutamate transporters in retinal ganglion cell survival following stimulation of NMDA receptor. *Curr Eye Res*. 2012;37:170–178.

Investigative Ophthalmology & Visual Science